Provenance analyses of silted sediments in Shenzhen Bay: Insights based on rare earth elements and stable isotopes

Qi Yan [a], Yaqing Liu [b], Cuilan Qu [c], Junting Song [b], Autif Hussain Mangi [b,d], Bing Zhang [c], Jin Zhou [b], Zhonghua Cai [b,*]

[a] *School of Life Science, Tsinghua University, Beijing, 100083, China*
[b] *The Institute for Ocean Engineering, Tsinghua Shenzhen International Graduate School (SIGS), Tsinghua University, Shenzhen 518055, Guangdong Province, China*
[c] *Shenzhen Institute of Quality & Safety Inspection and Research, 518055, China*
[d] *Institute of Biochemistry, University of Sindh Jamshoro 76080, Pakistan*

ABSTRACT

Shenzhen Bay (SZB) in southern China is a typical eutrophic area, with internal pollution from its sediments representing an important nutrient source. However, the transport paths and sources of sediments in SZB remain unclear, making it difficult to analyze the nutritional budget and propose effective sediment management strategies. To address this, we linked a sediment fingerprinting technique to a Bayesian mixing model (MixSIAR) and conducted provenance analyses. We collected particle samples from SZB sediment and surrounding areas, including the Shenzhen River (SZR), Pearl River Estuary (PRE), and the northern South China Sea (SCS). Two groups of natural tracers were measured to trace different phases of sediments: (1) C and N parameters for the fates of the organic phase of sediments, and (2) rare earth element (REE) patterns for the provenance of mineral fragments. The results showed that the concentrations of total organic C and total N were 0.89–1.44 % and 0.05–0.13 %, respectively. MixSIAR suggested that fluvial inputs from SZR and PRE contributed 46.6 % and 30.3 % of organic matter, respectively. The organic matter in the PRE mainly originated from sewage and the upper reaches of the Pearl River. The concentration range of REEs in SZB sediments was 153.12–480.09 mg/kg with clear enrichment for light REE. MixSIAR results showed that the mineral fragments mainly originated from the outer bay (SCS and PRE, which contributed 57.2 % and 32.7 %, respectively). These results indicate that organic pollution follows a different path from the inorganic base, which is mainly related to anthropogenic input from land. This study highlights that complex sediment transport processes and pollution intrusions from the Pearl River are the issues that must be considered for eutrophication restoration in SZB.

1. Introduction

Shenzhen has experienced substantial economic liftoff in the past 40 years, and is now one of the most densely urbanized regions worldwide and one of the main hubs of China's economic growth [1]. However, this was accompanied by the degradation of the

ecosystems of Shenzhen Bay (SZB), an estuary that has experienced severe eutrophication as a result of anthropogenic activities during urbanization [2]. Eutrophication poses various ecological threats to coastal environments, including harmful algal blooms [3], heavy metal pollution [4], and reduced biodiversity [5]. In 2021, the average concentrations of dissolved inorganic N (DIN) and ortho-phosphate P (PO_4^{3-}) were over 1.3 and 0.1 mg/L, respectively, in the inner Bay, which is rated Grade Four, the worst seawater grade in China [6]. Therefore, there is an urgent need to determine the root cause of eutrophication and develop sustainable governance for seawater quality.

The silted sediment has been proved as a key factor in eutrophication management and sustainable development of SZB. Previous study estimated the annual load of total N (TN) and total P (TP) in SZB and found point-source pollution accounted for 49.9–75.5 % and 60.4–87.6 % of TN and TP, respectively [7]. Long-term excessive pollution loads can lead to high pollutant enrichment in sediments [8]. Internal pollution from sediments across the water–sediment interface is also regarded as an important source of eutrophication in SZB. As a modelling study predicted, even complete elimination of terrigenous loads of DIN would only decrease the DIN content of the SZB by half [9]. Our previous study quantitatively confirmed that internal loading supplied 65 % and 69 % of total DIN and PO_4^{3-} input fluxes in SZB, which were 4.0×10^6 and 0.3×10^6 mol/d, respectively [10]. The silted sediment not only aggravates eutrophication, but also threatens vessel safety and brought an unfavorable perceptual experience for residents due to black-odor problem [11]. Therefore, the siltation and pollution were urgent problems ahead for the sustainable development of SZB.

Sediment transport paths and particle sources determine the basic principles of estuarine sediment governance [12,13]. Sediment fingerprinting is an increasingly used approach for provenance analysis of coastal and riverine sediments [14]. This approach employs a physicochemical tracer property that distinguishes source materials (e.g., sediment size, trace metals, and fallout radionuclides) and combines it with statistical tools to unmix potential contributions [15]. Most researchers select C and N parameters (mainly stable isotopes and atomic ratios), which are widely used as natural tracers, to determine the provenance of organic matter (OM) [16,17]. These parameters are closely related to the types of organic components in sediments and vary considerably in particular end-members of marine ecosystems [18]. For example, algae have a distinctive C/N ratio (4–10) compared to that of vascular plants, which is higher than 20 [19]. In anthropogenic emissions, marine OM is characterized by a relatively enriched $\delta^{13}C$ (−23 ‰ to −18 ‰) compared to terrestrial sources (−28 ‰ to −25 ‰) [20]. These chemical signatures have offered valuable insights for river basin and coastal management, as well as landscape conservation, in the Mississippi River Basin [21] and southeastern Brazil [22].

However, traditional single-organic tracer systems consider sediment particles as a whole and are too broad for assessing coastal pollution sources [14]. In coastal areas, the bioavailability of the organic phase makes it difficult to use organic parameters alone to trace other constituents [23]. The mineral base can determine the behavior of the water–sediment interface and affect internal pollution from sediments [24,25]. Most research has focused only on the organic phase, ignoring the distinguishable transportation processes of inorganic constituents due to size and weight [26] or low biodegradability [27]. This prevents us from developing management strategies for issues dominated by inorganic components like sedimentation and benthic nutrient release [28]. To avoid the one-sidedness of organic tracers, we used another natural tracer, rare earth elements (REEs), to aid in the determination of the provenance of SZB sediments. REEs consist of 17 elements, La–Lu, Sc, and Y, which are widely distributed in rocks, soil, and sediments [29]. During erosion and fluvial transportation of the source material, the contents and differentiation characteristics of REEs are mainly controlled by the source rock and can only be further changed via metamorphic, weathering, or environmental processes [30]. Therefore, the quantity and distribution patterns of REEs are exemplary indicators for identifying the mineral sources in sediments [31, 32]. For example, previous study found that light REEs (LREEs; including La, Ce, Pr, Nd, Sm, and Eu) were enriched in sediment samples and speculated that REE concentrations in offshore areas of the Shandong Peninsula were mainly controlled by continental inputs [33]. The above two natural tracers can provide information for distinguishing different sediment fragments. C and N parameters have been used to evaluate the sources of the OM deposited, whereas REE data focuses on the provenance of rock fragments. Such a combined fingerprinting system tracing two constituents separately will extend the discussion on discrepant sources of sediment fragments and is urgently needed for the development of corresponding SZB remediation policies.

To obtain more comprehensive and accurate source apportionment results, we introduced a new generation of geo-fingerprint tools, the MixSIAR Bayesian mixing model, to our study [34]. The MixSIAR Bayesian mixing model uses fixed and random effects as covariates to determine the contribution ratio of each source [17,35]. Simultaneously, using a Markov chain Monte Carlo (MCMC) algorithm, it repeatedly simulates the random sampling of source variables, thereby achieving reasonable assessments of the likelihood of source proportions. Compared to traditional end-member models, the MixSIAR Bayesian model incorporates all source and mixture sample data and can produce a more reliable statistical prediction [36].

To the best of our knowledge, less consideration has been given to the provenance analysis of SZB sediment particles. The only study based on hydrodynamic equations showed that a triangular region outside the Dasha Estuary had a heavy sediment load, and that these sediments originated from both terrigenous and marine inputs [37]. In this study, we attempted to identify the source of SZB sediments and trace the different constituents separately by combining the C/N ratio, stable C isotopes, and REE patterns. Accordingly, we collected suspended particle and sediment core samples from SZB and the surrounding areas. After analyzing the physicochemical characteristics of the sediments, the relative contribution of potential sources was assessed using the MixSIAR model and two sediment fragments (organic and detritus phases) were quantitatively tracked. We intended to analyze the transport processes and overall budget of the sediment, which can provide a new perspective on the heavy anthropogenic influence on SZB and aid in the discovery of better strategies for estuary management.

2. Materials and methods

2.1. Site description and sampling

SZB is a semi-enclosed shallow bay located on the east of the Pearl River Estuary (PRE; approximately 113°53′–114°05′E, 22°30′–22°39′N; Fig. 1a). It has a coastline of approximately 14 km and covers an estimated area of 89.5 km^2, with an average water depth of approximately 3.0 m. The salinity of the waters in Shenzhen Bay is around 18 to 22 psμ. The bay experiences irregular semidiurnal tidal currents throughout the year, predominantly rotating counterclockwise. Due to the unique shape, the average velocity of SZB remains relatively low, approximately 0.5 m/s. Over the last 40 years, SZB has become a typical eutrophic bay. Four rivers, namely, the Shenzhen River (SZR), Dasha River, Xiaosha River, and Yuen Long River, connect to the SZB. The freshwater entering the bay is mainly from SZR, which accounts for approximately 75 % of total freshwater inflow, with an average annual discharge of 5.3×10^8 m^3 [38]. The measured seabed data indicated that large volumes of sediment rapidly accumulated in a silted triangular area outside the Dasha River Estuary (Fig. 1b). Approximately 33 % of the triangular region is exposed during low tides [37]; therefore, we selected these areas as the study sites.

The sampling cruise was conducted in June 2020. Nine 75-cm-long independent sediment cores were collected from the silted area of SZB at 300-m intervals (designated as SZB1–SZB9; Fig. 1b) using a piston column sediment collector (length: 100 cm, diameter: 6 cm). The sediment cores were evenly divided into five layers by depth using single-use polypropylene tablets. Each layer was 15-cm thick and was used for geochemical parameter measurements, including REE, isotope, and elemental analyses. The average sedimentation rate of SZB was 2.58 cm/a over the past century, indicating that the 75-cm sediment section dated back to nearly 30 years [39]. Sediment particles were classified based on particle size distributions [11], and fine gravel (diameter: 2–5 mm), coarse sand (diameter: 0.3–2 mm), and fine sand (diameter: <0.3 mm) constituted approximately one-third of the total particles.

Furthermore, suspended sediment samples (SS) were obtained from the confluence of the PRE and SZB (Fig. 1b) utilizing a floating sediment trap equipped with eight distinct tubes designed for the collection of particles [40]. Surface sediments from the SZR estuary (0–10 cm in depth) were collected using a stainless-steel grab (SZR; Fig. 1b). The constitution and operating methods of the above-mentioned tools are provided in the Supplementary information (SI). All the samples were transferred to the laboratory in a cool tank containing ice. Prior to chemical analysis, the sediments and particles were freeze-dried using a freeze dryer (Alpha 1–2 LD; Martin Christ Instrument Co., Germany) and ground into a fine powder through a 2-mm sieve.

2.2. Organic C/N and isotopic composition analysis

The pretreated sample (2 g dry weight) was weighed and treated with 15 mL 1 M HCl for 24 h. The sediments were then centrifuged (4000 rpm for 10 min), repeatedly rinsed with deionized water until the supernatant was neutral, and freeze-dried [41]. The dried samples were used for subsequent analyses. Total organic C (TOC) and TN contents were analyzed using an elemental analyzer (Flash EA-HT 1112; Thermo Scientific, Germany) with an analytical precision of <0.5 %. The C/N ratios were calculated using corrections for atomic mass [42]. Stable isotope analyses (δ^{13}C) were performed using a Delta V Advantage isotope ratio mass spectrometer coupled with a Flash HT 2000 Elemental Analyzer (Thermo Fisher Scientific Inc., USA). The δ^{13}C values were expressed using the delta notation (δ) in units per mil (‰), and defined as δ^{13}C: δ (‰) = $(R_{samples} - R_{standard})/R_{standard} \times 1000$, where R represents the isotopic ratio (^{13}C/^{12}C) of the samples and the standard (Vienna Peedee Belemnite and atmospheric N$_2$ were used for C and N, respectively). The analytical precision calculated from the standards systematically interspersed in the analytical batches was 0.1 ‰.
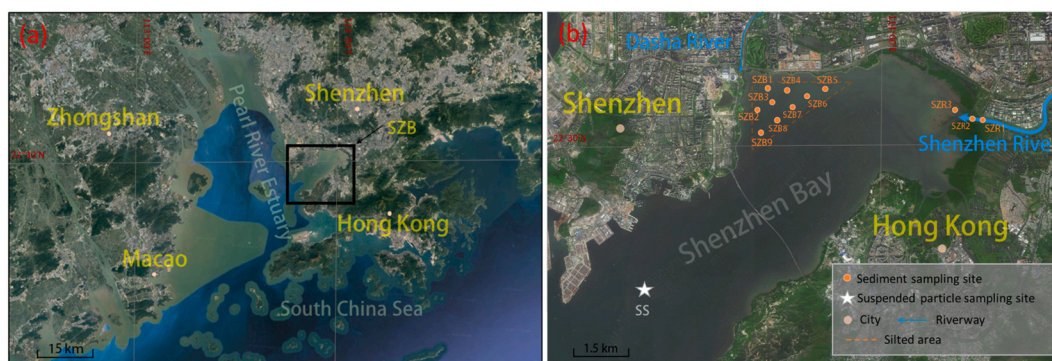
Fig. 1. Location of Shenzhen Bay (SZB) (a) and sampling sites in SZB (b). The black frame symbol represents the relative location of SZB in the Pearl River Estuary. The general area of the triangular silted area is framed by dotted lines. Blue curves indicate freshwater input from rivers. Orange dots represent sampling sites in SZB (SZB1–SZB9) and Shenzhen River (SZR) (SZR1–SZR3). The star symbol denotes the site where sediments samples (SS) in the joint area were collected.

2.3. Analysis of REE concentrations

Fourteen REEs (La, Ce, Pr, Nd, Sm, Eu, Gd, Tb, Dy, Ho, Er, Tm, Yb, and Lu) in the freeze-dried samples were measured using a triple quadrupole inductively coupled-plasma mass spectrometer (Agilent 8800 ICP-MS, USA). Specifically, approximately 0.1 g frozen-dried sediment sample was weighed, dissolved in HF–HNO$_3$ (1:1, v:v), and subsequently redried at 190 °C for 48 h. After cooling, the solid residues were redissolved in 3 mL 50 % HNO$_3$, and then dried at 150 °C for an additional 8 h. The detection limits of REEs were 0.001–0.01 μg/kg and the relative measurement error was <2 %.

To eliminate the Oddo–Harkins effect, we introduced chondrite (CI) and Post-Archean Australian Shale (PAAS), which have been widely used to compare samples of coastal sediments [43,44], to normalize REE patterns. In this study, we used the measured values from meteoritic samples [45]. Additionally, the REE anomalies were calculated based on the chondrite-normalized pattern, referring to the enrichment level of some elements relative to their neighbors in the REE [43]. The Ce and Eu anomalies (δCe and δEu, respectively) were quantified using the following equations:

$$\delta Ce = Ce_{CI}/(La_{CI} \times Pr_{CI})^{0.5}$$

$$\delta Eu = Eu_{CI}/(Sm_{CI} \times Gd_{CI})^{0.5}$$

2.4. Statistical analysis

2.4.1. Bayesian mixture model

The MixSIAR package in R language (version 4.2.2) was used to establish three models for OM and rock fragment provenance [35]. Generally, we analyzed the OM source of SZB sediment using a nested model, which combined Models A and B. The geochemical tracer of the nested model included the δ^{13}C and C/N ratios according to previous methods [17,34]. Because of the isotopic fractionation of microbial activity, deep sediments (<15 cm) were not included in this model. Additionally, we set Model C to compare the relative contributions of the rock fragments of SZB sediments from three potential sources: PRE, SZR, and marine sources (South China Sea, SCS). The tracers contained 14 REEs, and the configurations and model references for the aforementioned types are listed in Table 1. The MCMC parameters were set as follows: chain length = 1,00,000 and number of chains = 3. The convergence of the models was evaluated using the Gelman–Rubin diagnostic method.

Table 1
Model configurations.

Model configuration	Model A	Model B	Model C
Mixtures	Surface sediments of SZB	Suspended sediments of SS	Different sediment layers in depth of SZB
Parameter	δ13C and C/N atomic ratio	δ13C and C/N atomic ratio	concentration of 14 rare earth elements, including La, Ce, Pr, Nd, Sm, Eu, Gd, Tb, Dy, Ho, Er, Tm, Yb, and Lu
Source 1	Sediments of SZR	Sewage [17] δ13C: −25.3 ± 2.8 ‰ C/N: 12.5 ± 0.8	Sediments of SZR
Source 2	Suspended sediments of SS	Reaches of Pearl River [46] δ13C: −23.9 ± 1.0 ‰ C/N: 13.3 ± 1.4	Reaches of Pearl River [44]
Source 3	Surface sediment from the continental shelf of the northern South China sea [46] δ13C: −20.8 ± 0.4 ‰ C/N: 7.5 ± 1.1	Surface sediment from the continental shelf of the northern South China sea [46] δ13C: −20.8 ± 0.4 ‰ C/N: 7.5 ± 1.1	Surface sediment from the continental shelf of the northern South China sea (NSCS) [47]
Source 4	Marine phytoplankton [36] δ13C: −18.5 ± 1.4 ‰ C/N: 8.9 ± 1.2	Marine phytoplankton [36] δ13C: −18.5 ± 1.4 ‰ C/N: 8.9 ± 1.2	\
Source 5	C3 plant [36] δ13C: −29.1 ± 1.8 ‰ C/N: 22.7 ± 11.6	C3 plant [36] δ13C: −29.1 ± 1.8 ‰ C/N: 22.7 ± 11.6	
Source 6	C4 plant [36] δ13C: −13.1 ± 0.5 ‰ C/N: 24.6 ± 9.4	C4 plant [36] δ13C: −13.1 ± 0.5 ‰ C/N: 24.6 ± 9.4	
Prior	Uninformative/generalist	Uninformative/generalist	Uninformative/generalist
Discrimination	0	0	0
Residual	error	error	error
Process	error	error	error
MCMC chain length	100,000	100,000	100,000

2.4.2. Data analysis

One-way analysis of variance (ANOVA) was used to determine the significant differences in isotopic and REE characteristics among different depth layers and sources using SPSS 18.0 software (IBM SPSS Statistics for Windows).

3. Results

3.1. TOC, TN, C/N, and $\delta^{13}C$ of sediment samples

The elemental compositions of the collected samples were first presented to show the basic chemical characteristics. Fig. S1 shows the vertical distributions of TOC, TN, C/N, and $\delta^{13}C$ in SZB sediments. The TOC and TN contents of SZB sediments ranged from 0.89 % to 1.44 % and 0.05 %–0.13 %, respectively. The atomic C/N ratios analyzed in this study ranged from 10.39 to 22.46. One-way ANOVA revealed few significant differences in TOC, TN, and C/N ratio among the sampling sites ($p \geq 0.1$). However, significant differences were noted among the sediment sections at different depths ($p < 0.01$). Vertically, the 0–15 cm layer had highest average TOC (1.28 ± 0.14 %) and TN (0.12 ± 0.01 %) values. These two parameters first decreased, and then increased at a depth of 60–75 cm (TOC: 1.08 ± 0.10 %; TN: 0.11 ± 0.00 %). A strong positive correlation was observed between TOC and TN in the sediment samples (TN% = 0.111, TOC% = 0.0301, $R^2 = 0.50$); however, the C/N ratio showed the opposite trend to TOC and TN ($P < 0.01$).

The TOC and TN of the sediment particles from SS and SZR were significantly higher than those of the SZB samples, respectively ($p < 0.05$). The average contents of TOC in SS and SZR were 1.46 ± 0.23 % and 1.72 ± 0.17 %, respectively, while the TN contents of the two sites were 0.18 ± 0.01 % and 0.20 ± 0.01 %, respectively. The TOC and TN of the SCS sediment were 0.73 ± 0.12 % and 0.13 ± 0.01 %, respectively [46].

The $\delta^{13}C$ in the SZB sediment samples ranged from -25.85 ‰ to -23.24 ‰, with an average value of -24.53 ± 0.64 ‰ (n = 45). The $\delta^{13}C$ values fluctuated significantly among the different layers with depth (one-way ANOVA, $p < 0.01$); however, the variation in sampling sites was not significant ($p \geq 0.1$). Generally, the $\delta^{13}C$ values increased with depth, where the 0–15 cm layer had the lowest $\delta^{13}C$ value (-25.31 ± 0.32 ‰). The average $\delta^{13}C$ value in SCS sediment was -21.42 ± 0.07 ‰ [46].

3.2. Provenance of OM in SZB sediments

To identify the source of OM in SZB, the scatter diagrams of the samples and potential sources were drawn based on the C/N and $\delta^{13}C$ value (Fig. 2). The dominant plants in south China, C3 plants, use the Calvin photosynthetic pathway and have a much lower $\delta^{13}C$ value (-29.10 ± 1.80 ‰) than C4 plants, which use the Hatch–Slack pathway (-13.10 ± 0.50 ‰) [36]. Marine planktons may use HCO_3^- (1 ‰) and atmospheric CO_2 (-7‰) for photosynthesis and therefore have higher $\delta^{13}C$ than C3 plants [42]. In comparison, sediment particles had higher $\delta^{13}C$ values than C3 plants, and significant differences in $\delta^{13}C$ values were identified among sediment particle sources (SZR, SS, and SZB) using one-way ANOVA ($p < 0.001$, $R^2 = 0.63$). The sediment samples from the upper reaches of the Pearl River (PRE) had elemental characteristics that were most similar to SZB sediments. In particular, the SZB sediments at 60–75 cm depth had nearly identical positions. Additionally, SS and SZR were tightly focused around SZB sediments.

Nested Bayesian models (Models A and B) were used to estimate the relative contributions of different OM sources in the surface sediments (at a depth of 15 cm) of SZB. In this nested model, an SS (PRE end-member) was used as a source in Model A and a mixture in Model B. This design enabled a more accurate assessment of the fate of OM because PRE is influenced by many factors and should not be regarded as the ultimate source of OM.
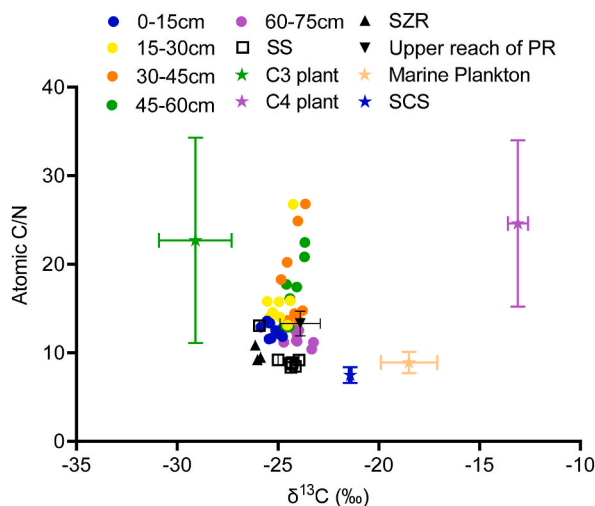
Fig. 2. C/N and $\delta^{13}C$ of sediments in Shenzhen Bay (SZB) and other the potential sources. Error bars indicate the standard deviation of each member. SZB sediments were collected from the following depths: 0–15, 15–30, 30–45, 45–60, and 60–75 cm.

The bay ecosystem had four sources of OM: C3 and C4 plants, marine phytoplankton (MP), and marine-source particles (MS). In Model A, two specific sources were considered for the hydrodynamic analysis: (1) particle inputs from PRE (SS) and (2) particle inputs from the SZR riverway. The convergence of all the variables was assessed and met the Gelman (<1.05) and Geweke criteria. Probability distributions showed low correlation among different sources (Fig. 3a). SZR and PRE (SS) may be the two major OM contributors in SZB, with average contributions of 46.6 % and 30.3 %, respectively (Fig. 3b). C3 plants contributed approximately 14.0 % of OM in surface sediments, while the contributions of C4 plants, SCS, and marine phytoplankton were very small (all <4 %).

In Model B, SS was used as the mixture. Based on similar previous research [17,46], sewage and OM from the upper reaches of the Pearl River were selected as potential sources of PRE sediments. These variables had satisfactory convergence, which met the Gelman (<1.05) and Geweke criteria. Similarly, a low correlation was observed among the different sources because no coefficient varied beyond ± 0.3 (Fig. 3c). The output of the MixSIAR suggested that sewage contributed the majority of OM in PRE sediments, with an average contribution value of 46.3 % (Fig. 3d). This was followed by the upper reaches of the Pearl River (33.7 %) and SCS (17.4 %). The other three sources contributed little to OM in SS (all <2 %).
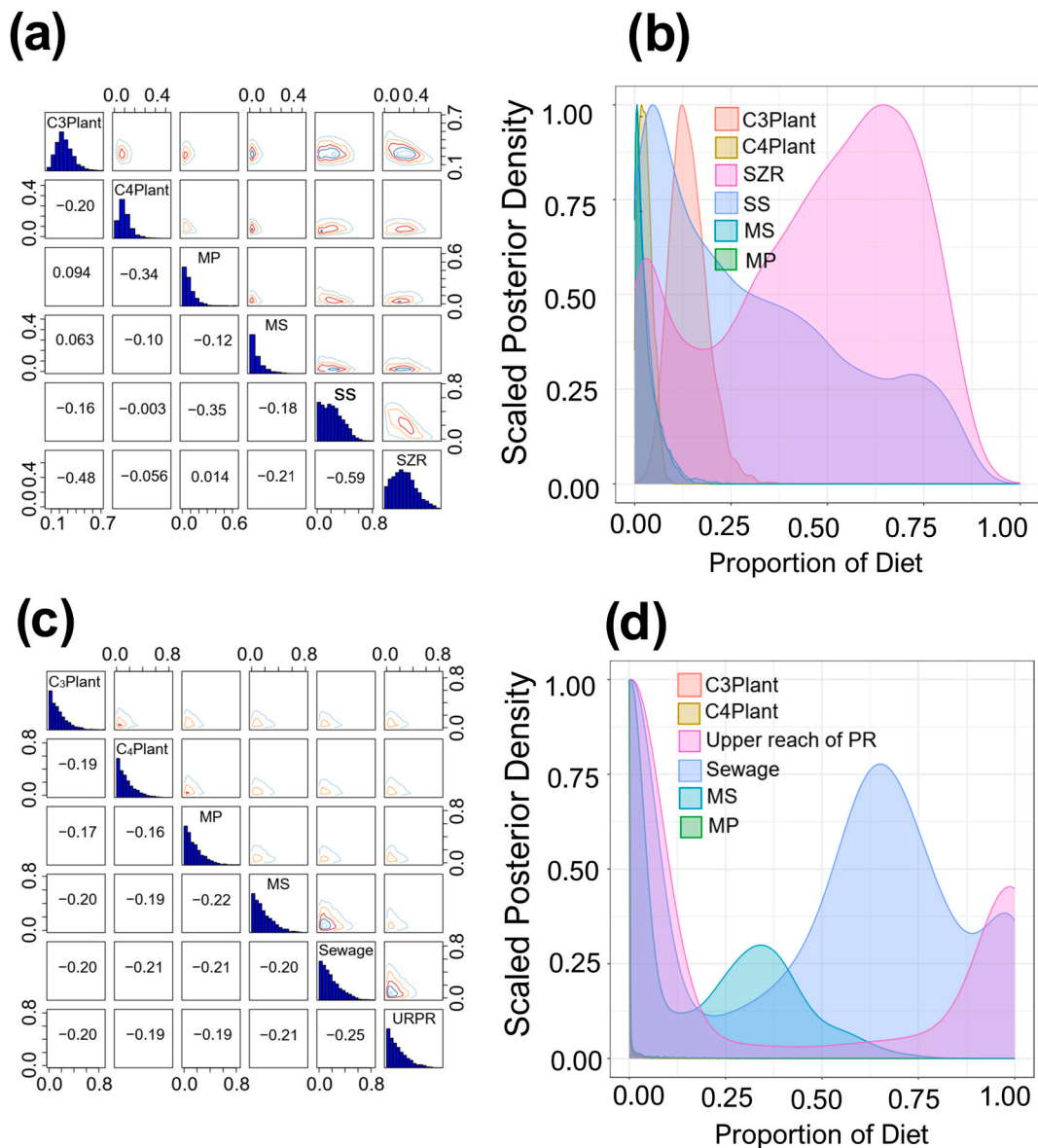
Fig. 3. Output of the nested model (combined Models A and B) based on MixSIAR. Images (a) and (c) show the matrix plot of potential sources in Models A and B, respectively. Histograms indicate probability distributions for each source and numeric value is the correlation between the contributions of the two sources. Contour diagram shows the joint probability of both sources. Scaled relative probability (y-axis) of proportional source contribution (x-axis) for (b) Shenzhen Bay (SZB) sediment and (d) SS. MS means marine sources (sediments in SCS). MP means marine phytoplanktons.

3.3. REE concentrations and patterns

The REE concentrations of SZB, SS, and SZR sediments are listed in Table 2. The mean REE values in all samples were in the following order: Ce > La > Nd > Pr > Gd > Sm > Dy > Er > Yb > Eu > Ho > Tb > Tm > Lu. In SZB, the total REE concentration of sediment samples ranged from 153.12 mg/kg to 480.09 mg/kg, with an average value of 274.40 ± 63.98 mg/kg. One-way ANOVA revealed significant differences in the total REEs among the different layers at different depths (p = 0.07). Sediments from the 15–30-cm layer had the lowest abundances of total REEs (255.47 ± 35.70 mg/kg). The 45–60-cm layer had the highest abundance of total REEs (296.98 ± 83.92 mg/kg). The ratio of LREE to heavy REE (HREE) ranged from 10.32 to 13.53, with an average of 12.09. In contrast, the SS and samples from SZR had much lower REE abundances than those from SZB, with average values of 169.97 ± 11.65 mg/kg and 155.16 ± 7.45 mg/kg, respectively ($p \leq 0.01$). The average ratios of LREE to HREE were 9.86 and 7.69, respectively.

Two-normalized patterns were used to compare different sources of SZB sediments. The chondrite-normalized pattern indicated minor differences among the various types of samples (Fig. 4a). Differences in the enrichment of LREE compared to that of HREE and a slight Eu anomaly were evident in all samples. These trends are consistent with typical patterns of marginal sea sediments worldwide [33]. However, the PAAS-normalized pattern highlighted the differences among the different samples (Fig. 4b): all metal elements were enriched in PRE particles but deprived in SCS samples. SZB sediments were characterized by enrichment in LREE and deprivation in HREE. Only two elements (Pr and Lu) were enriched in the SS.

3.4. Provenance of rock fragment in SZB sediments

REE anomalies have been widely used for provenance differentiation. In this study, Ce and Eu anomalies were selected for the scatter plots to distinguish the supply relationship (Fig. 5). Samples of SZB sediments were dispersed, except for samples collected at a depth of 60–75 cm. Similarly, SCS sediments had a wide range of δ^{Ce} values. SS and SCS largely overlapped with SZB sediment, indicating high similarity among the samples. SS was surrounded by other samples, suggesting that it was influenced by many sources

Table 2
Rare earth element (REE) concentration in Shenzhen Bay (SZB) sediments and other sources. The data represent mean values and standard deviations of the mean.

mg/kg	SZB sediments in different depth (n = 9)					SS (n=3)	Surface sediment of SZR (n = 3)	Surface sediment from NSCS (n = 273)	Suspended particles in PRE (n = 6)
	0–15 cm	15–30 cm	30–45 cm	45–60 cm	60–75 cm				
La	67.91 ± 11.82	66 ± 8.58	69.89 ± 18.73	74.23 ± 20.97	66.26 ± 10.77	36.92 ± 2.68	32.86 ± 1.55	33.72 ± 11.71	89.66 ± 33.15
Ce	117.02 ± 20.48	110.73 ± 16.29	116.63 ± 40.78	131.75 ± 39.57	128.66 ± 22.15	71.53 ± 5.02	61.19 ± 3.72	65.61 ± 24.02	193.45 ± 73.19
Pr	14.04 ± 2.12	13.22 ± 2.05	13.81 ± 3.85	15.09 ± 4.18	13.79 ± 2.65	9.31 ± 0.71	8.56 ± 0.34	7.43 ± 2.84	23.51 ± 9.57
Nd	40.92 ± 5.73	37.94 ± 5.71	40.18 ± 12.28	43.31 ± 12.21	41.11 ± 7.66	30.15 ± 2.40	28.27 ± 1.09	26.89 ± 10.28	85.91 ± 34.99
Sm	7.73 ± 1.14	7.01 ± 1.10	7.32 ± 2.33	8.09 ± 2.26	7.28 ± 1.92	5.46 ± 0.43	5.51 ± 0.25	5.24 ± 1.97	14.62 ± 6.21
Eu	1.41 ± 0.24	1.26 ± 0.20	1.37 ± 0.35	1.53 ± 0.55	1.58 ± 0.26	0.95 ± 0.08	0.92 ± 0.04	0.97 ± 0.4	2.24 ± 0.87
Gd	7.73 ± 1.04	7.08 ± 1.22	7.49 ± 2.49	8.29 ± 2.31	7.76 ± 1.49	4.54 ± 0.34	5.17 ± 0.27	4.40 ± 1.65	11.63 ± 4.81
Tb	1.08 ± 0.16	1.08 ± 0.11	1.06 ± 0.29	1.09 ± 0.3	1.01 ± 0.25	0.83 ± 0.10	0.98 ± 0.11	0.76 ± 0.28	1.80 ± 0.76
Dy	5.18 ± 0.82	4.58 ± 0.64	4.81 ± 1.47	5.50 ± 1.57	5.10 ± 0.95	3.8 ± 0.26	4.48 ± 0.24	4.07 ± 1.52	11.59 ± 5.06
Ho	1.09 ± 0.18	0.95 ± 0.13	1.00 ± 0.31	1.16 ± 0.35	1.02 ± 0.28	0.81 ± 0.06	0.95 ± 0.06	0.81 ± 0.3	2.25 ± 1.00
Er	2.89 ± 0.48	2.56 ± 0.32	2.69 ± 0.76	3.14 ± 0.95	2.89 ± 0.51	2.34 ± 0.17	2.69 ± 0.17	2.41 ± 0.9	6.17 ± 2.73
Tm	0.41 ± 0.07	0.35 ± 0.05	0.37 ± 0.12	0.45 ± 0.14	0.41 ± 0.08	0.37 ± 0.03	0.41 ± 0.03	0.34 ± 0.13	0.83 ± 0.35
Yb	2.51 ± 0.44	2.23 ± 0.25	2.34 ± 0.60	2.80 ± 0.92	2.53 ± 0.41	2.32 ± 0.20	2.49 ± 0.17	2.27 ± 0.83	4.78 ± 1.98
Lu	0.56 ± 0.08	0.47 ± 0.10	0.44 ± 0.06	0.53 ± 0.03	0.30 ± 0.16	0.65 ± 0.07	0.70 ± 0.03	0.33 ± 0.12	0.89 ± 0.40
ΣREE	270.47 ± 43.08	255.47 ± 35.7	269.39 ± 83.84	296.98 ± 83.92	279.70 ± 48.24	169.97 ± 11.65	155.16 ± 7.45	155.26 ± 56.55	449.32 ± 174.24
ΣLREE	249.03 ± 40.56	236.16 ± 33.21	249.20 ± 78.00	274.01 ± 77.71	258.68 ± 44.64	154.31 ± 10.93	137.30 ± 6.62	139.85 ± 50.94	409.4 ± 157.56
ΣHREE	21.44 ± 2.97	19.31 ± 2.57	20.19 ± 5.90	22.96 ± 6.27	21.02 ± 3.73	15.66 ± 0.94	17.85 ± 0.95	15.40 ± 5.72	39.93 ± 16.88
L/H	11.62 ± 0.90	12.22 ± 0.43	12.28 ± 0.54	11.94 ± 0.56	12.33 ± 0.60	9.86 ± 0.48	7.69 ± 0.22	9.11 ± 1.00	10.48 ± 0.88
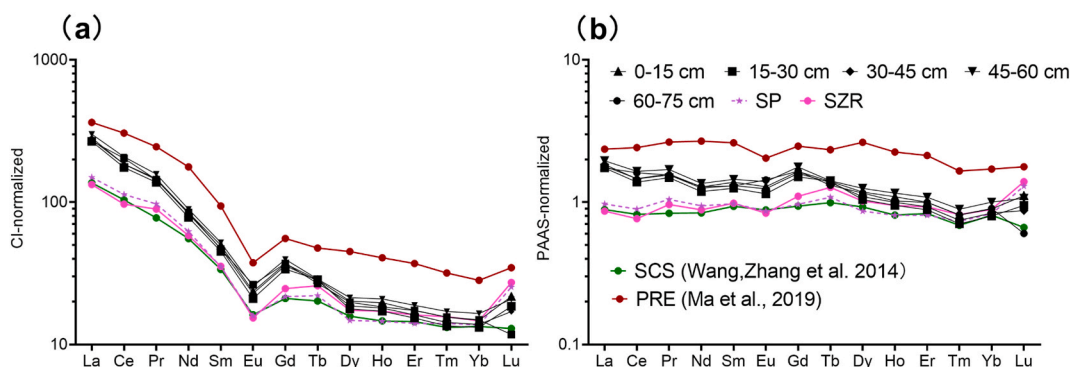
Fig. 4. Rare earth element (REE) patterns of Shenzhen Bay (SZB) sediments and the potential sources. Abundances are normalized to the recommended mean value of chondrites (a) and Post-Archean Australian Shale (PAAS) (b). SZB sediments were collected form the following depths: 0–15, 15–30, 30–45, 45–60, and 60–75 cm. The star represents normalized patterns for sediments samples (SS). Three potential sources are represented as dots with different colors: Shenzhen River (SZR; pink), South China Sea (SCS; green), and Pearl River Estuary (PRE; red).
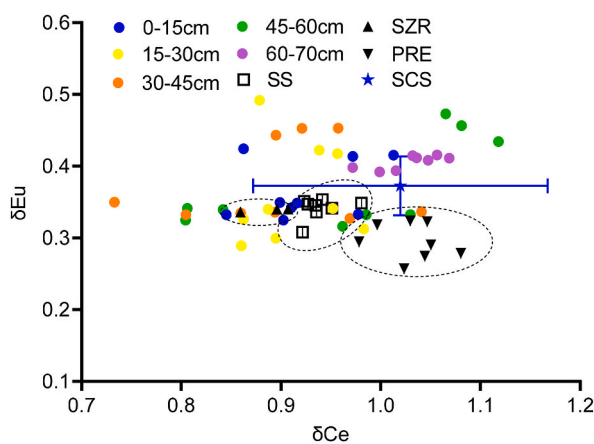
Fig. 5. Values of the and Pr/Pr × anomalies of sediments from Shenzhen Bay (SZB) in and the potential sources. The anomalies of rare earth elements (REEs) are calculated based on the chondrite-normalized pattern. SZB sediments were collected form the following depths: 0–15, 15–30, 30–45, 45–60, and 60–75 cm.

and could not be regarded as an endmember. Accordingly, in the Bayesian model, we selected the SCS, SZB, and PRE as potential sources of SZB rock fragments.

MixSIAR first analyzes the variability and dependency among sources. Histograms based on probability distributions indicate a strong positive correlation between the contributions of SZR and PRE, with a numerical value of −0.81 (Fig. 6a). The pair correlations between SCS and the other two sources were weak and moderate with coefficients of −0.23 and −0.39. Fig. 6b–d shows scaled relative probability of proportional source contribution for different sediment layers in the order of 0–15, 15–30, 30–45, 45–60, and 60–75 cm, respectively. The rock fragments were likely to have originated mainly from SCS and PRE. The relative proportions of SCS and PRE were approximately stable among different layers, with mean values of 57.2 % and 32.7 %, respectively. This indicates that the contribution of SCS was highest in the 60–75-cm layer at 65.6 %. With increasing depth, the proportion of PRE source showed no observable changes. However, the contribution of SZR widely ranged from 2.9 % to 15.2 %, and maximum and minimum values appeared in surface (0–15 cm) and bottom (60–75 cm) layers.

4. Discussion

4.1. MixSIAR helped effectively identify the sediment sources of SZB

In this study, we introduced MixSIAR, a Bayesian mixing model in R, to separately track two sediment components. The advantage of MixSIAR is that it treats all the model parameters probabilistically and incorporates a separate residual error term [48]. Although these steps can reduce the likelihood of unrepresentative data, relative uncertainty remains regarding element fractionation in particle transit, which may present a weakness in the application of all MixSIAR methods. Therefore, it was necessary to verify whether the predicted values agreed with the observed data.
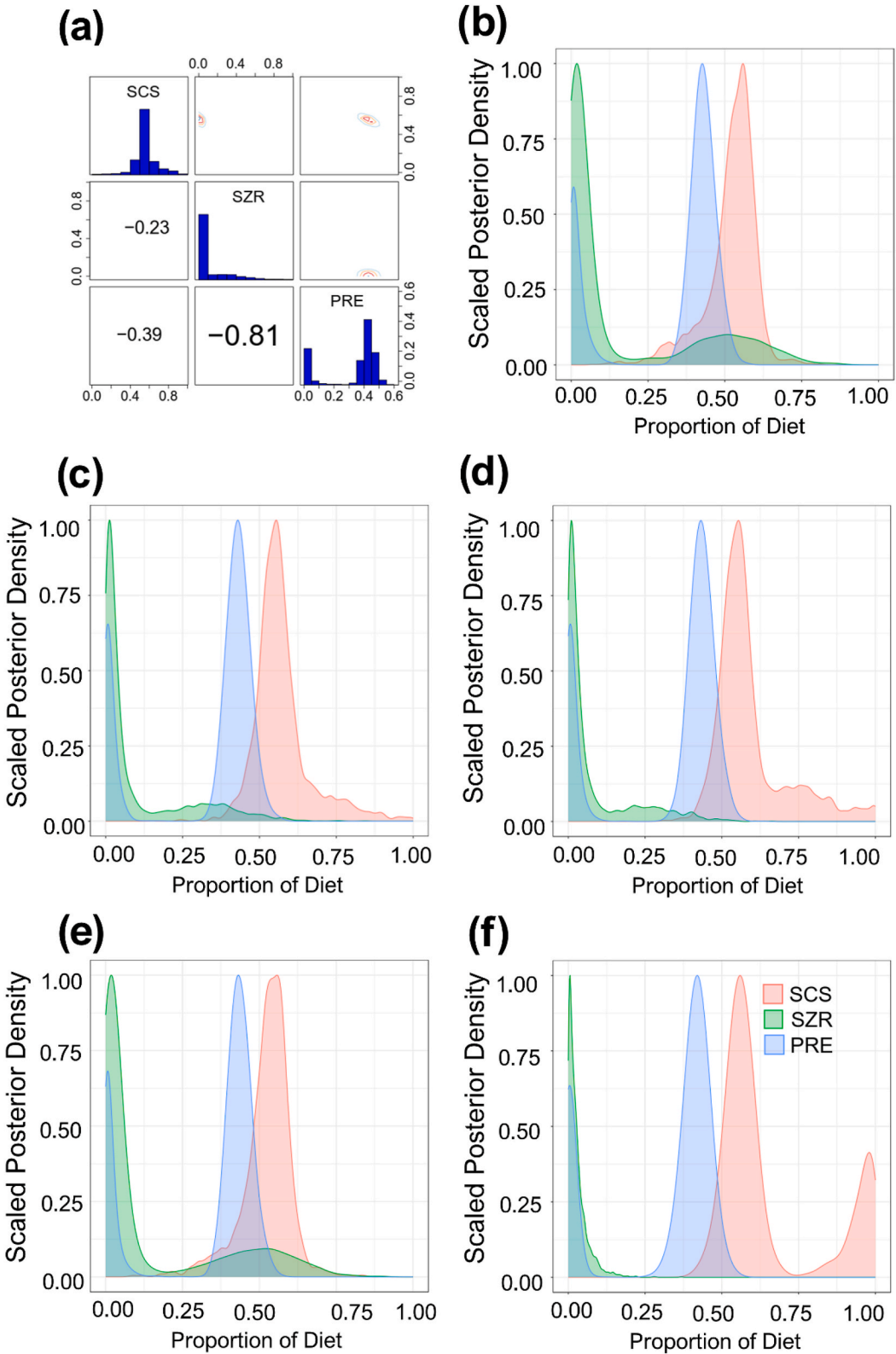
(caption on next page)

Fig. 6. Output of the Model C based on MixSIAR. (a) Matrix plot of three sources (South China Sea [SCS], Pearl River Estuary [PRE], and Shenzhen River [SZR]). Histograms indicate probability distributions for each source, and the numeric values represent the correlation between contributions of the pair sources. Contour diagram shows the joint probability of both sources. Images (b–d) show scaled relative probability (y-axis) of proportional source contribution (x-axis) for different sediment layers in the order of 0–15, 15–30, 30–45, 45–60, and 60–75 cm, respectively.

Calibration coefficients (CCs) are basic calculations used to verify the validity and effectiveness of stimulated values [49]. When we calculated CCs (multiple sources by their respective contribution ratios) and incorporated sources in the mixture space, we produced C values that were exactly equal to those of the observed value (Fig. 7a). The offset (percentage of the difference and observed value) of $\delta^{13}C$ was only 2.39 % and that of C/N value was 28.40 %. This difference reflects the specificity and variability of the C/N values and the biochemical transformation of sediment storage [50]. The C/N parameters of original sources had high variation: the coefficients of variation (CVs) of C/N of C3 and C4 plants were 38.21 % and 51.10 %, respectively. Considering the noise introduced by creating random values, the output was acceptable.

In contrast, REE tracers showed lower end-member uncertainty because using multiplex fingerprint properties is thought to reduce uncertainty [51,52]. In Model C, MixSIAR used 14 relatively independent tracers to identify sources and provided reliable results within an acceptable range (Fig. 7b–f). The average offsets of all elements in different layers were 14.82 %, 22.05 %, 20.13 %, 13.48 %, and 21.36 %, much lower than the CVs of elemental distributions of SCS and PRE, which were over 35 % on average.

Furthermore, different types of REEs have different offset ranges. HREEs (except for Gd and Tb) deviated more from the real
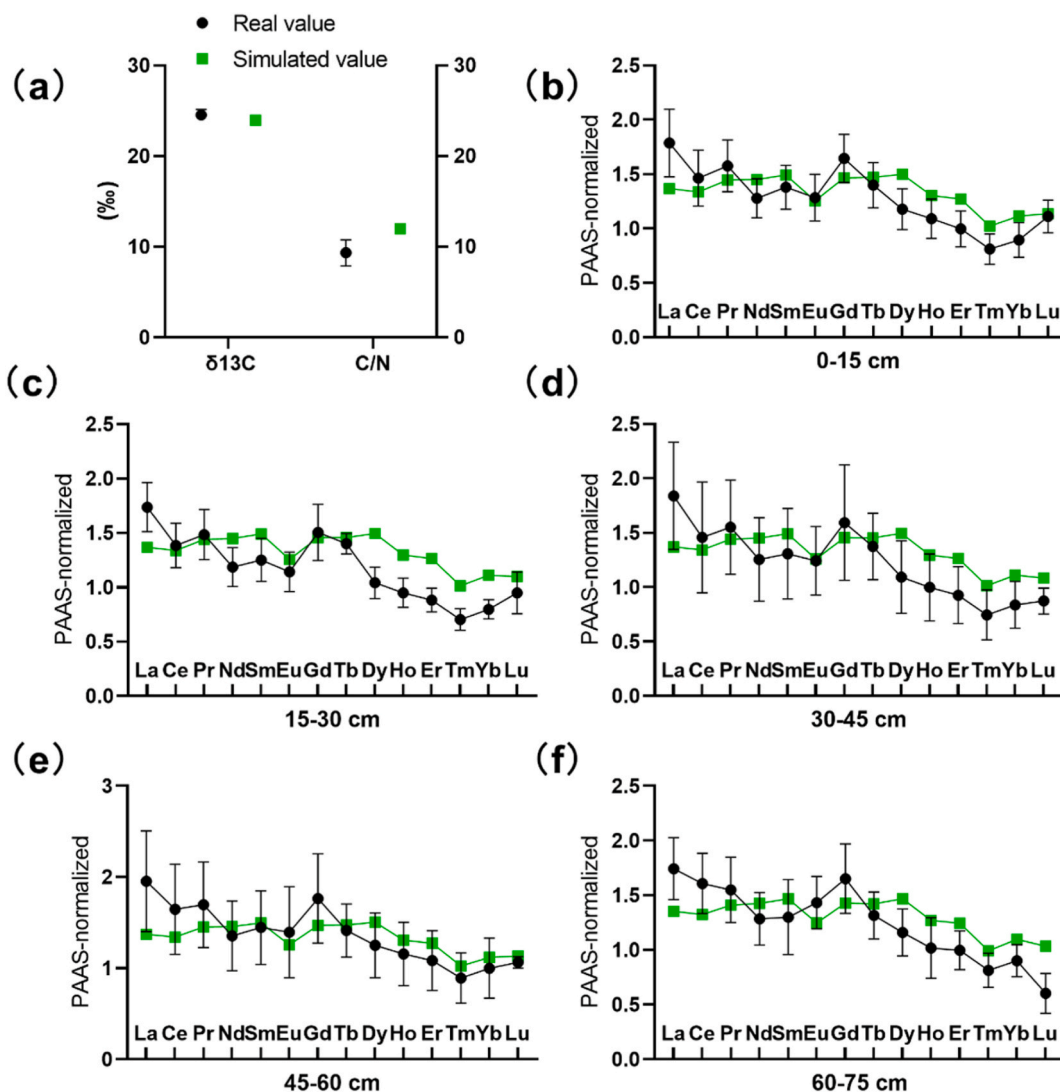
Fig. 7. Comparison between the observed and MixSIAR-simulated data. Simulated values are multiplicative, which equals the sum of the tracer value of each source multiplied by its corresponding contribution based on MixSIAR. Black dots represent the observed values, whereas green squares represent the simulated values. Image (a) used data from Model A. Images (b–d) used data from Model C.

average value than LREEs. According to the output of Model C, most of the HREEs were overrated. The total offsets of these HREEs were greater than 24 %, with Dy having the largest offset of 30.91 %. This difference is associated with the different fates of LREEs and HREEs; generally, LREEs are more readily complexed by solid particles [53], whereas HREEs have a stronger affinity toward dissolved ligands [54]. This caused a poor fit of the HREEs between the observed and simulated values; therefore, it is necessary to calculate the fractionation coefficients of the different types of REEs for more precise modes. Taken together, although non-conservative REE transport is not completely understood, our results support the use of MixSIAR with appropriate offsets for provenance differentiation in SZB. A quantitative and high-precision evaluation of MixSIAR is not easy, and further research is necessary.

4.2. Different fragments of sediments have different transport paths

In open-sea areas, the transportation of most OM is considered to be bound to inorganic base components due to OM–mineral interactions [55]. However, in estuaries and coastal areas, the association between two fragments is uncertain [56]. A previous study emphasized the stabilization between transported OM and sediment generation [57]; however, uncoupling between organic and inorganic fragments in sediments occurs frequently due to several factors, such as photosynthesis [58], solubilization and sorption [59], and OM disaggregation [60].

Similarly, from the results of Model A, we found that the OM of SZB sediments, but not inorganic fragments, mainly originated from SZR and PRE. In other words, fluvial transport influenced by extensive anthropogenic activity was the dominant pathway for OM. Visually, SZB sediment is unnaturally black with an unpleasant smell, suggesting a high OM content (e.g., sulfur compounds), and is always affected by the urbanization [61]. Both the Pearl River and SZR are surrounded by densely populated districts and have undergone severe eutrophication; with the Pearl River receiving approximately 7 and 2 billion m^3 of domestic wastewater and industrial wastewater annually, respectively, and treated and untreated wastewater is discharged into the PRE and its adjacent waters [62]. In the SZR, 71 % of the area had poor water quality in the past, with a chemical oxygen demand exceeding 13 mg/L and TN exceeding 10 mg/L [63]. This transport provides mass OM to the bay, and some OM is converted into marine sediment particles through thermal transformation and sorption–aggregation [64]. Additionally, bacteria can assimilate OM and silt into sediment [65].

Fluvial OM was found to be the dominant source of sediment, in contrast to the previous findings [42,66]. These two studies indicated that, in some shallow lakes, algae were the main source of OM because terrigenous inputs enhanced C sequestration. However, in the SZB, the fluvial inputs in organic form (46.6 %) were significantly greater than the primary production from marine phytoplankton (2.3 %). Consistent with this interpretation, C/N in SZB sediment (12.23, on average) was much higher than that of marine phytoplankton (8.9, on average), suggesting the influence of land organic inputs. Notably, nutrient supplementation from SZR was not accompanied by the transport of rock particles, as SZR only contributed approximately 15 % to SZB rock fragments. This is because most river-driven particle OM have a lower density and are therefore easier to move with the current. In contrast, owing to interception facilities and silted riverbeds, large particles have difficulty moving with the flows and are generally intercepted before entering SZB [67].

In comparison, marine sediment brought by tides was the source of sediment mineral constituents (57.2 %) but with extremely low OM inputs (<3 %). This is consistent with the previous findings, which reported the similarity of rock types between SCS and SZB sediment particles and highlighted the potential particle transfer relationship [68]. The transportation of these SCS sediments to SZB is highly likely to be facilitated by tidal exchange water, as extensive evidence supports the dominance of tides in the local water budget. The tide fluxes were 37.57×10^6 and 21.63×10^6 m^3/d in the wet and dry seasons, respectively. This value is approximately ten times higher than that of terrigenous freshwater flows [10]. Using Delft 3D models, other researcher found that at maximum ebb and flood, suspended sediment particles from the outer bay (SCS and PRE) were trapped in the area outside Dasha Estuary because of its shallow water depth [37]. Therefore, these marine particles formed an inorganic sediment basement in SZB.

4.3. Theoretical support for SZB restoration

MixSIAR results showed that terrigenous inputs (SZR and PRE) contributed over 75 % of OM in SZB sediments. Although the sampling points in this study do not fully cover the entire SZB, all samples come from the areas with the highest sedimentation rates, which can reflect the characteristics of particle input over a long period in the past. Previous studies have confirmed that pollution originating from river sources contributes to sediment contamination [10,38]. Therefore, reducing the anthropogenic emissions of the surrounding cities is crucial for SZB restoration. Governments have realized this, and remediation efforts have been made to reduce pollution in the target river waters. For example, since the 2000s, five wastewater purification plants have been established in Shenzhen, and approximately 90 % of TP and 65 % of TN can currently be removed after treatment [38]. Moreover, governments are pushing ahead with bans on P detergents and effectively controlling TP inputs to local waters. However, sediment pollution always lags in response to a decrease in input stress; thus, reducing accumulated nutrients and achieving self-purification requires a relatively long time period [69]. Moreover, the highly polluted background of PRE may potentially undermine the efficiency of these efforts. Our study showed that particles from PRE contributed 30 % of the OM in the sediment, which aligns with the fact that the PRE effectively transports a substantial amount of organic particles through tides. It was determined that PRE exerted significant control over the flow exchange in SZB, particularly during the wet season [70]. This influence facilitated the intrusion of pollutants from the Pearl River. Additionally, when we sought to pinpoint the source of organic matter (OM) in PRE, Model B indicated that anthropogenic factors predominantly shaped the destiny of PRE-derived OM, with sewage contributing to 46.3 % of the total. Sewage mostly originated from PRE–urban agglomeration (including nine cities located in the lower reaches of the Pearl River), which accounts for 79.1 % of the total GDP of Guangdong Province [71]. We emphasize that multiregional coalitions across the upstream and downstream regions would be

more effective in pollution control of SZB. For example, emission permit trading has been regarded as a powerful tool to reduce total sewage discharge and the number of wastewater over-discharged cities in the Songhua River Basin [72]. Policymakers should consider both socioeconomic and ecological implications when proposing restoration strategies.

The transportation of mineral components is associated with sedimentation. Some researchers have proposed solving the internal pollution problem using dredging operations [73], which appears to be the most straightforward approach. Sediment removal will reduce internal pollution and ameliorate eutrophication. However, dredging decreases taxonomic richness and damages the estuarine ecosystem [74]. SZB is a large habitat for estuarine species, particularly migratory birds, and dredging seriously harms habitats and interferes with bird settlement. Another major problem is the treatment and dumping of dredged sediments containing various contaminants [75]. More importantly, our study showed that tides from the outer bay caused continuous sediment deposition into the inner bay. From the results of Model C, in terms of silted volume, over 80 % of volume was from the outer bay. Although SZR contributed mineral components of only 2.9 % in earlier years, it has increased to 15.2 % in recent times. With increasing silting years, the water depth becomes shallower and sediment deposition becomes heavier [37]. The tidal transport from the sea source will inevitably result in continuous sediment deposition, leading to repeated dredging operations, which requires considerable manpower and resources and cannot fundamentally handle this problem. Therefore, dredging is not the first choice for pollution control in SZB. Administrators must consider these complex considerations when designing restoration and management approaches for sediment eutrophication problems.

5. Conclusion

In this study, we investigated the sediment profiles of organic C, N, and REEs. Then, the MixSIAR Bayesian mixing model was used to identify the contributions from potential sources. The model results showed that SZR and PRE contributed 46.6 % and 30.3 % of OM in SZB, respectively. However, over 57 % of the rock fragments in the sediments originated from marine sources (SCS). The uncoupling of the organic and inorganic fragments indicated that human activities altered the natural process of particle accumulation and increased the flux of organic matter into the sediments of SZB. Our research findings validate the important role of the PRE in influencing nutrient budgets within SZB. Although this study had a limited sampling scope, collecting only the sediment-dense inner bay area, the results proved that particles from marine tides lead to persistent accumulation issues that cannot be fully resolved by dredging. Therefore, it is essential to consider the environmental effects of all complex factors in the restoration and management of SZB.

Data availability statement

Data included in article/supp. Material/referenced in article.

CRediT authorship contribution statement

Qi Yan: Writing – original draft, Investigation, Data curation, Conceptualization. **Yaqing Liu:** Investigation. **Cuilan Qu:** Validation, Methodology, Investigation. **Junting Song:** Supervision, Investigation. **Autif Hussain Mangi:** Methodology, Investigation. **Bing Zhang:** Methodology. **Jin Zhou:** Writing – review & editing, Methodology. **Zhonghua Cai:** Writing – review & editing, Supervision, Methodology, Funding acquisition, Conceptualization.

Declaration of competing interest

The authors declare that they have no known competing financial interests or personal relationships that could have appeared to influence the work reported in this paper.

Acknowledgments

Appendix A. Supplementary data

Supplementary data to this article can be found online at https://doi.org/10.1016/j.heliyon.2023.e21559.

References

[1] R. Hu, The state of smart cities in China: the case of shenzhen, Energies 12 (2019), https://doi.org/10.3390/en12224375.

[2] Z. Mu, X. Shen, M. Chai, H. Xu, R. Li, G. Qiu, Characteristics of water quality changes in the futian mangrove national natural reserve, Acta Sci Nat Univ Pekin 54 (2018) 137–145, https://doi.org/10.13209/j.0479-8023.2017.138, in Chinese.

[3] L.I. Li, L. Song-Hui, A 30-year retrospective analysis over the detrimental algal blooms in Guangdong coastal areas, J. Saf. Environ. 9 (2009) 83–86, in Chinese.

[4] Y. Shi, M. Li, B. Li, J. Wei, G. Wu, Spatial and temporal distribution of heavy metals in the sediment of Shenzhen bay, Mar. Environ. Sci. 36 (2017) 186 (in Chinese).

[5] L.Z. Cai, J.S. Hwang, H.U. Dahms, S.J. Fu, X.W. Chen, C. Wu, Does high organic matter content affect polychaete assemblages in a shenzhen bay mudflat, China, J. Marine Sci. Technol.-Taiwan 21 (2013) 274–284, https://doi.org/10.6119/jmst-013-1223-5.

[6] E.P.D. Hong Kong, Annual Report of Marine Water Quality in Hong Kong, 2022. https://www.epd.gov.hk/epd/english/environmentinhk/water/hkwqrc/waterquality/marine-2.html.

[7] C. Zhao, S. Zhang, X. Mao, Variations of annual load of TN and TP in the deep bay watershed, Shenzhen, Environ. Sci. 35 (2014) 4111–4117, in Chinese.

[8] K.-W. Man, J. Zheng, A.P.K. Leung, P.K.S. Lam, M.H.-W. Lam, Y.-F. Yen, Distribution and behavior of trace metals in the sediment and porewater of a tropical coastal wetland, Sci. Total Environ. 327 (2004) 295–314, https://doi.org/10.1016/j.scitotenv.2004.01.023.

[9] Y.-P. Wan, X.-Z. Mao, Simulation and evaluation on TIN and PO_4^{3-} -P reduction in Deep Bay, China, Huan jing ke xue, in Chinese 32 (2011) 384–391.

[10] Q. Yan, T. Cheng, J. Song, J. Zhou, C.-C. Hung, Z. Cai, Internal nutrient loading is a potential source of eutrophication in Shenzhen Bay, China, Ecol. Indicat. 127 (2021), 107736, https://doi.org/10.1016/j.ecolind.2021.107736.

[11] Q. Yan, J.T. Song, J. Zhou, Y.L. Han, Z.H. Cai, Biodeposition of oysters in an urbanized bay area alleviates the black-malodorous compounds in sediments by altering microbial sulfur and iron metabolism, Sci. Total Environ. (2022) 817, https://doi.org/10.1016/j.scitotenv.2021.152891.

[12] P.N. Owens, Sediment behaviour, functions and management in river basins, in: Sustainable Management of Sediment Resources, 2008, pp. 1–29.

[13] R.R. Twilley, S.J. Bentley, Q. Chen, D.A. Edmonds, S.C. Hagen, N.S.N. Lam, C.S. Willson, K.H. Xu, D. Braud, R.H. Peele, et al., Co-evolution of wetland landscapes, flooding, and human settlement in the Mississippi River Delta Plain, Sustain. Sci. 11 (2016) 711–731, https://doi.org/10.1007/s11625-016-0374-4.

[14] P.N. Owens, W.H. Blake, L. Gaspar, D. Gateuille, A.J. Koiter, D.A. Lobb, E.L. Petticrew, D.G. Reiffarth, H.G. Smith, J.C. Woodward, Fingerprinting and tracing the sources of soils and sediments: earth and ocean science, geoarchaeological, forensic, and human health applications, Earth Sci. Rev. 162 (2016) 1–23, https://doi.org/10.1016/j.earscirev.2016.08.012.

[15] J.P. Laceby, O. Evrard, H.G. Smith, W.H. Blake, J.M. Olley, J.P.G. Minella, P.N. Owens, The challenges and opportunities of addressing particle size effects in sediment source fingerprinting: a review, Earth Sci. Rev. 169 (2017) 85–103, https://doi.org/10.1016/j.earscirev.2017.04.009.

[16] Q.J. Guo, C.Y. Wang, R.F. Wei, G.X. Zhu, M. Cui, C.P. Okolic, Qualitative and quantitative analysis of source for organic carbon and nitrogen in sediments of rivers and lakes based on stable isotopes, Ecotoxicol. Environ. Saf. 195 (2020), https://doi.org/10.1016/j.ecoenv.2020.110436.

[17] H. Xiao, C. Mao, S. Wang, Z. Jia, W. Rao, Seasonal variation and provenance of organic matter in the surface sediments of the three gorges reservoir: stable isotope analysis and implications for agricultural management, Sci. Total Environ. 870 (2023), 161886, https://doi.org/10.1016/j.scitotenv.2023.161886.

[18] B. Liu, Y. He, Y. Zhang, Y. Sun, Y. Wang, D. He, Natural and anthropogenic organic matter cycling between coastal wetlands and rivers: a case study from Liao River Delta, Estuarine, Coastal and Shelf Science 236 (2020), 106610, https://doi.org/10.1016/j.ecss.2020.106610.

[19] D. Maksymowska, P. Richard, H. Piekarek-Jankowska, P. Riera, Chemical and isotopic composition of the organic matter sources in the gulf of gdansk (southern baltic sea), estuarine, Coastal and Shelf Science 51 (2000) 585–598, https://doi.org/10.1006/ecss.2000.0701.

[20] H.Y. Xiao, C.Q. Liu, Identifying organic matter provenance in sediments using isotopic ratios in an urban river, Geochem. J. 44 (2010) 181–187, https://doi.org/10.2343/geochemj.1.0059.

[21] Z. Xu, P. Belmont, J. Brahney, A.C. Gellis, Sediment source fingerprinting as an aid to large-scale landscape conservation and restoration: a review for the Mississippi River Basin, J. Environ. Manag. 324 (2022), https://doi.org/10.1016/j.jenvman.2022.116260.

[22] R.S. Carreira, L.G.M.S. Cordeiro, D.R.P. Oliveira, A. Baêta, A.L.R. Wagener, Source and distribution of organic matter in sediments in the SE Brazilian continental shelf influenced by river discharges: an approach using stable isotopes and molecular markers, J. Mar. Syst. 141 (2015) 80–89, https://doi.org/10.1016/j.jmarsys.2014.05.017.

[23] K. Vercruysse, R.C. Grabowski, R.J. Rickson, Suspended sediment transport dynamics in rivers: multi-scale drivers of temporal variation, Earth Sci. Rev. 166 (2017) 38–52, https://doi.org/10.1016/j.earscirev.2016.12.016.

[24] E. Kristensen, G. Penha-Lopes, M. Delefosse, T. Valdemarsen, C.O. Quintana, G.T. Banta, What is bioturbation? The need for a precise definition for fauna in aquatic sciences, Mar. Ecol. Prog. Ser. 446 (2012) 285–302, https://doi.org/10.3354/meps09506.

[25] C.G. Shao, Y. Sui, D.L. Tang, L. Legendre, Spatial variability of surface-sediment porewater pH and related water-column characteristics in deep waters of the northern South China Sea, Prog. Oceanogr. 149 (2016) 134–144, https://doi.org/10.1016/j.pocean.2016.10.006.

[26] D.E. Walling, P.N. Owens, B.D. Waterfall, G.J.L. Leeks, P.D. Wass, The particle size characteristics of fluvial suspended sediment in the Humber and Tweed catchments, UK, Sci. Total Environ. 251 (2000) 205–222, https://doi.org/10.1016/s0048-9697(00)00384-3.

[27] R.G. Keil, L.M. Mayer, P.D. Quay, J.E. Richey, J.I. Hedges, Loss of organic matter from riverine particles in deltas, Geochem. Cosmochim. Acta 61 (1997) 1507–1511, https://doi.org/10.1016/S0016-7037(97)00044-6.

[28] Y. Zhang, P. Li, X.J. Liu, L. Xiao, E.H. Chang, Y.Y. Su, J.W. Zhang, Z. Liu, Sediment and soil organic carbon loss during continuous extreme scouring events on the Loess Plateau, Soil Sci. Soc. Am. J. 84 (2020) 1957–1970, https://doi.org/10.1002/saj2.20169.

[29] A.R. Chakhmouradian, F. Wall, Rare earth elements: minerals, mines, magnets (and more), Elements 8 (2012) 333–340, https://doi.org/10.2113/gselements.8.5.333.

[30] F. Wall, Rare earth elements, in: D. Alderton, S.A. Elias (Eds.), Encyclopedia of Geology, second ed., Academic Press, Oxford, 2021, pp. 680–693.

[31] D. Bi, S. Zhai, D. Zhang, C. Xiu, X. Liu, X. Liu, L. Jiang, A. Zhang, Geochemical characteristics of the trace and rare earth elements in reef carbonates from the xisha islands (south China sea): implications for sediment provenance and paleoenvironment, J. Ocean Univ. China 18 (2019) 1291–1301, https://doi.org/10.1007/s11802-019-3790-0.

[32] G. Xu, J. Liu, X. Kong, J. Zhang, J. Qiu, Rare earth elements in surface sediments of western south yellow sea and their provenance implications, Mar. Geol. Quat. Geol. 32 (2012) 11–17, https://doi.org/10.3724/sp.J.1140.2012.01011.

[33] Y.T. Zhu, R. Bao, L.H. Zhu, S.H. Jiang, H.B. Chen, L.J. Zhang, Y.F. Zhou, Investigating the provenances and transport mechanisms of surface sediments in the offshore muddy area of Shandong Peninsula: insights from REE analyses, J. Mar. Syst. 226 (2022), https://doi.org/10.1016/j.jmarsys.2021.103671.

[34] L. Duan, H. Zhang, F. Chang, D. Li, Q. Liu, X. Zhang, F. Liu, Y. Zhang, Isotopic constraints on sources of organic matter in surface sediments from two north–south oriented lakes of the Yunnan Plateau, Southwest China, J. Soils Sediments 22 (2022) 1597–1608, https://doi.org/10.1007/s11368-022-03191-2.

[35] B.C. Stock, A.L. Jackson, E.J. Ward, A.C. Parnell, D.L. Phillips, B.X. Semmens, Analyzing mixing systems using a new generation of Bayesian tracer mixing models, PeerJ 6 (2018), https://doi.org/10.7717/peerj.5096.

[36] Z. Li, S. Wang, X. Nie, Y. Sun, F. Ran, The application and potential non-conservatism of stable isotopes in organic matter source tracing, Sci. Total Environ. 838 (2022), 155946, https://doi.org/10.1016/j.scitotenv.2022.155946.

[37] W.R. Wu, L.L. Wang, X.Y. Lei, Y. Zheng, J. Wei, X.Z. Mao, Sustainable estuarine governance based on artificial island scheme for a highly anthropogenic influenced Shenzhen Bay, China, J. Hydrol. 616 (2023), https://doi.org/10.1016/j.jhydrol.2022.128784.

[38] Y. Zhou, L. Wang, Y. Zhou, X.-Z. Mao, Eutrophication control strategies for highly anthropogenic influenced coastal waters, Sci. Total Environ. 705 (2020), 135760, https://doi.org/10.1016/j.scitotenv.2019.135760.

[39] L. Zhang, Z. Cui, Y. Wang, Z. Xia, J. Gao, S. Ma, Grain size variation and heavy metals distribution during last hundred years under the impact of human activities in the inner Lingdingyang bay of the Pearl River estuary, Mar. Geol. Quat. Geol. 36 (2016) 27–42.

[40] C.C. Hung, C.W. Tseng, G.C. Gong, K.S. Chen, M.H. Chen, S.C. Hsu, Fluxes of particulate organic carbon in the East China Sea in summer, Biogeosciences 10 (2013) 6469–6484, https://doi.org/10.5194/bg-10-6469-2013.

[41] A.J. Midwood, T.W. Boutton, Soil carbonate decomposition by acid has little effect on delta C-13 of organic matter, Soil Biol. Biochem. 30 (1998) 1301–1307, https://doi.org/10.1016/s0038-0717(98)00030-3.

[42] L. Zeng, S. Mcgowan, G.E.A. Swann, M.J. Leng, X. Chen, Eutrophication has a greater influence on floodplain lake carbon cycling than dam installation across the middle Yangtze region, J. Hydrol. 614 (2022), 128510, https://doi.org/10.1016/j.jhydrol.2022.128510.

[43] V. Hatje, K.W. Bruland, A.R. Flegal, Increases in anthropogenic gadolinium anomalies and rare earth element concentrations in San Francisco bay over a 20 Year record, Environ. Sci. Technol. 50 (2016) 4159–4168, https://doi.org/10.1021/acs.est.5b04322.

[44] L. Ma, D.H. Dang, W. Wang, R.D. Evans, W.-X. Wang, Rare earth elements in the Pearl River Delta of China: potential impacts of the REE industry on water, suspended particles and oysters, Environ. Pollut. 244 (2019) 190–201, https://doi.org/10.1016/j.envpol.2018.10.015.

[45] R.A. Schmitt, R.H. Smith, J.E. Lasch, A.W. Mosen, D.A. Olehy, J. Vasilevskis, Abundances of the 14 rare-earth elements, scandium, and yttrium in meteoritic and terrestrial matter, Geochem. Cosmochim. Acta 27 (1963) 577–622, https://doi.org/10.1016/0016-7037(63)90014-0.

[46] B. He, M. Dai, W. Huang, Q. Liu, H. Chen, L. Xu, Sources and accumulation of organic carbon in the Pearl River Estuary surface sediment as indicated by elemental, stable carbon isotopic, and carbohydrate compositions, Biogeosci. Discuss. 7 (2010), https://doi.org/10.5194/bgd-7-2889-2010.

[47] S.H. Wang, N. Zhang, H. Chen, L. Li, W. Yan, The surface sediment types and their rare earth element characteristics from the continental shelf of the northern south China sea, Continent. Shelf Res. 88 (2014) 185–202, https://doi.org/10.1016/j.csr.2014.08.005.

[48] R.J. Cooper, T. Krueger, An extended Bayesian sediment fingerprinting mixing model for the full Bayes treatment of geochemical uncertainties, Hydrol. Process. 31 (2017) 1900–1912, https://doi.org/10.1002/hyp.11154.

[49] A.I. Guerrero, T.L. Rogers, Evaluating the performance of the Bayesian mixing tool MixSIAR with fatty acid data for quantitative estimation of diet, Sci. Rep. 10 (2020), 20780, https://doi.org/10.1038/s41598-020-77396-1.

[50] W.I. Ford, J.F. Fox, D.T. Mahoney, G. Degraves, A. Erhardt, S. Yost, Backwater confluences of the Ohio river: organic and inorganic fingerprints explain sediment dynamics in wetlands and marinas, J. Am. Water Resour. Assoc. 56 (2020) 692–711, https://doi.org/10.1111/1752-1688.12850.

[51] A. Brosinsky, S. Foerster, K. Segl, H. Kaufmann, Spectral fingerprinting: sediment source discrimination and contribution modelling of artificial mixtures based on VNIR-SWIR spectral properties, J. Soils Sediments 14 (2014) 1949–1964, https://doi.org/10.1007/s11368-014-0925-1.

[52] B. Liu, D.E. Storm, X.J. Zhang, W. Cao, X. Duan, A new method for fingerprinting sediment source contributions using distances from discriminant function analysis, Catena 147 (2016) 32–39, https://doi.org/10.1016/j.catena.2016.06.039.

[53] L. Melluso, P. Censi, G. Perini, L. Vasconcelos, V. Morra, F. Guerreiro, L. Bennio, Chemical and isotopic (C, O, Sr, Nd) characteristics of the Xiluvo carbonatite (central-western Mozambique), Mineral. Petrol. 80 (2004) 201–213, https://doi.org/10.1007/s00710-003-0027-z.

[54] H. Elderfield, M.J. Greaves, The rare-earth elements in sea-water, Nature 296 (1982) 214–219, https://doi.org/10.1038/296214a0.

[55] T.M. Blattmann, Z. Liu, Y. Zhang, Y. Zhao, N. Haghipour, D.B. Montluçon, M. Plötze, T.I. Eglinton, Mineralogical control on the fate of continentally derived organic matter in the ocean, Science 366 (2019) 742–745, https://doi.org/10.1126/science.aax5345.

[56] S. Pulley, I. Foster, P. Antunes, The uncertainties associated with sediment fingerprinting suspended and recently deposited fluvial sediment in the Nene river basin, Geomorphology 228 (2015) 303–319, https://doi.org/10.1016/j.geomorph.2014.09.016.

[57] W.I. Ford, J.F. Fox, E. Pollock, Reducing equifinality using isotopes in a process-based stream nitrogen model highlights the flux of algal nitrogen from agricultural streams, Water Resour. Res. 53 (2017) 6539–6561.

[58] C. Kendall, S.R. Silva, V.J. Kelly, Carbon and nitrogen isotopic compositions of particulate organic matter in four large river systems across the United States, Hydrol. Process. 15 (2001) 1301–1346, https://doi.org/10.1002/hyp.216.

[59] P.J. Hernes, A.C. Robinson, A.K. Aufdenkampe, Fractionation of lignin during leaching and sorption and implications for organic matter "freshness", Geophys. Res. Lett. 34 (2007), https://doi.org/10.1029/2007gl031017.

[60] J. Fox, W. Ford, K. Strom, G. Villarini, M. Meehan, Benthic control upon the morphology of transported fine sediments in a low-gradient stream, Hydrol. Process. 28 (2014) 3776–3788, https://doi.org/10.1002/hyp.9928.

[61] J.X. Cao, Q. Sun, D.H. Zhao, M.Y. Xu, Q.S. Shen, D. Wang, Y. Wang, S.M. Ding, A critical review of the appearance of black-odorous waterbodies in China and treatment methods, J. Hazard Mater. 385 (2020), https://doi.org/10.1016/j.jhazmat.2019.121511.

[62] X.Z. Peng, S.S. Xiong, W.H. Ou, Z.F. Wang, J.H. Tan, J.B. Jin, C.M. Tang, J. Liu, Y.J. Fan, Persistence, temporal and spatial profiles of ultraviolet absorbents and phenolic personal care products in riverine and estuarine sediment of the Pearl River catchment, China, J. Hazard Mater. 323 (2017) 139–146, https://doi.org/10.1016/j.jhazmat.2016.05.020.

[63] X. Tong, Y. Wang, X. Liu, Y. Zhang, Pollution characteristics analysis and control measures of Shenzhen River, China water & wastewater, in Chinese) 36 (2020) 52–59.

[64] N. Jiao, G.J. Herndl, D.A. Hansell, R. Benner, G. Kattner, S.W. Wilhelm, D.L. Kirchman, M.G. Weinbauer, T. Luo, F. Chen, et al., Microbial production of recalcitrant dissolved organic matter: long-term carbon storage in the global ocean, Nat. Rev. Microbiol. 8 (2010) 593–599, https://doi.org/10.1038/nrmicro2386.

[65] J. Zhang, H. He, J. Hu, J. Yang, Control strategy of water pollution in the Shenzhen River, Res. Environ. Sci. 18 (2005) 40–44, in Chinese).

[66] Y. Wu, J. Zhang, S.M. Liu, Z.F. Zhang, Q.Z. Yao, G.H. Hong, L. Cooper, Sources and distribution of carbon within the Yangtze River system, Estuar. Coast Shelf Sci. 71 (2007) 13–25, https://doi.org/10.1016/j.ecss.2006.08.016.

[67] X. Wu, S. Gao, M. Wu, Analysis on historical genesis of Shenzhen River estuary and suggestion on its comprehensive regulation, Water Resour. Hydropower Eng. 46 (2015) 87–91, in Chinese).

[68] M. Wu, L. Shao, X. Pang, J. Liang, Characteristics of clay mineral assemblage in northern South China sea continental margin and its geological implications, J. Tongji Univ. Nat. Sci. 42 (2014) 630–635, https://doi.org/10.3969/j.issn.0253-374x.2014.04.021.

[69] B. Wang, M. Xin, Q. Wei, L. Xie, A historical overview of coastal eutrophication in the China Seas, Mar. Pollut. Bull. 136 (2018) 394–400, https://doi.org/10.1016/j.marpolbul.2018.09.044.

[70] Y. Yang, T.F.M. Chui, The role of the Pearl River flow in Deep Bay hydrodynamics and potential impacts of flow variation and land reclamation, J. Hydro-environ. Res. 34 (2021) 1–10, https://doi.org/10.1016/j.jher.2020.11.001.

[71] Z. Zhang, J. Peng, Z. Xu, X. Wang, J. Meersmans, Ecosystem services supply and demand response to urbanization: a case study of the Pearl River Delta, China, Ecosystem Services 49 (2021), 101274, https://doi.org/10.1016/j.ecoser.2021.101274.

[72] L. Wanhong, L. Fang, W. Fan, D. Maiqi, L. Tiansen, Industrial water pollution and transboundary eco-compensation: analyzing the case of Songhua River Basin, China, Environ. Sci. Pollut. Control Ser. 27 (2020) 34746–34759, https://doi.org/10.1007/s11356-019-07254-9.

[73] M. Zhang, W. Wang, Y. Zhao, G. Liu, Laboratory determination of nonlinear compressibility and parameters of dredged fill in Shenzhen bay, J Cent South Univ, Sci Technol 45 (2014) 3596–3601, in Chinese).

[74] N. Mallick, K.B. Johnson, C.A. Jacoby, The effect of environmental dredging of muck on an assemblage of benthic amphipods, J. Mar. Sci. Eng. 11 (2023), https://doi.org/10.3390/jmse11020444.

[75] N. Manap, N. Voulvoulis, Environmental management for dredging sediments - the requirement of developing nations, J. Environ. Manag. 147 (2015) 338–348, https://doi.org/10.1016/j.jenvman.2014.09.024.